89

A Shallow Water Model Distributed Using Domain Decomposition

Elías Kaplan

1 Introduction

The aim of the present work is the study of the astronomic and storm tidal currents in the Río de la Plata ($35°S, 54°W$). The hydrodynamic equations for shallow water in two dimensions, obtained by vertical integration of the Navier-Stokes equations that express the laws of mass and momentum conservation, are numerically solved employing a Leendertse scheme [LL78, Bor85].

Using the divide-and-conquer method of domain decomposition (**DD**) as the means of parallelization of the numerical solver we obtained a better response in terms of model speed and output detail thanks to flexibility in accommodating local refinement [GK92]. This allows near real-time operation of the model, coupled with transport-diffusion numerical models, for tidal prediction in ocean engineering applications.

The computation is performed in a cluster of high end workstations, communicated by message passing through a FDDI network using PVM [GBD$^+$93]. The computational domain is divided into blocks and a domain partitioner was developed to ensure a good load balancing.

2 The Shallow Water Model

Equations

The shallow water model is formed by the bidimensional unsteady equations of mass (2.1) and momentum (2.2) conservation, obtained by depth averaging Navier-Stokes [GKV$^+$92, KVR92]:

---

0 CeCal, Engineering School, Montevideo, Uruguay (elias@fing.edu.uy)
1 With a grant of the Conicyt-Uruguay, supported also by project ITDC'94-European Union.
Ninth International Conference on Domain Decomposition Methods
Editor Petter E. Bjørstad, Magne S. Espedal and David E. Keyes

$$\frac{\partial \eta}{\partial t} + \nabla \cdot (H\vec{V}) = 0, \tag{2.1}$$

$$\frac{\partial \vec{V}}{\partial t} + (\vec{V}\cdot\nabla)\vec{V} - 2(\vec{\Phi} \times \vec{V}) + g\nabla\eta + \frac{g\vec{V}\left\|\vec{V}\right\|}{{C_h}^2 H} + \frac{\vec{\tau_s}}{\rho H} + \varepsilon\Delta\vec{V} = 0, \tag{2.2}$$

where η is the elevation of the water above the mean level and $\vec{V} = (u, v, 0)$ is the velocity in the axis coordinates (x, y, z). Moreover, H is the depth of the water, g is the gravity acceleration, $\vec{\Phi} = (0, 0, \omega)$ is the angular velocity, $-2(\vec{\Phi} \times \vec{V})$ is the Coriolis force, C_h is the Chezy coefficient, ρ is the sea water density, $\vec{\tau_s} = (\tau_{sx}, \tau_{sy}, 0)$ is the wind stress at the sea surface and ε is the coefficient for turbulent viscosity.

Advective processes (corresponding to the terms $\vec{V}\cdot\nabla\vec{V}$) are dominant in atmospheric and oceanic circulation systems governed by shallow waters equations, while diffusive effects are important only in boundary layer regions [Net92]. Any numerical model working on those equations should treat advective effects accurately.

Discretization

A finite difference scheme is employed with a staggered mesh, implicit in space and explicit with splitting in the time domain. This *Arakawa class C grid* [Ark88] has good conservative properties and is also well suited to the **DD** method with overlapped regions as employed here [AL80].

Figure 1 Distribution of the dependent variables on a two-dimensional grid.

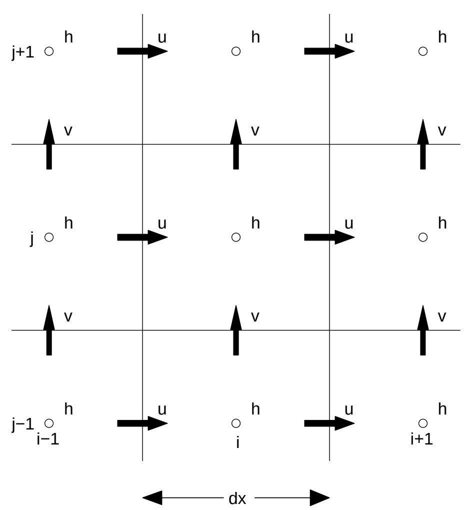

Boundary Conditions

The different types of boundary conditions to impose are [AQS94]:

1. At coastlines, zero normal velocity.
2. Normal velocity is prescribed at boundaries modeling inflow from rivers.
3. Surface elevation is prescribed at south oceanic boundary, modeling a wave that enters the computational domain. Prediction of this elevation is taken from oceanic models [Sch83, Ray93].
4. Open boundary condition to simulate tidal surges that leave the computational domain [RC87]. The criterion used in this development is a variation of the Sommerfeld radiation condition (eq. 2.3):

$$\eta_t + c^x \eta_x + c^y \eta_y = 0. \tag{2.3}$$

   Here $\vec{c} = (c^x, c^y)$ and $|\vec{c}| = \sqrt{gH}$ is the wave celerity. The wave at this boundary has the same direction as the water velocity and a sense that lets the surges leave the computational domain.
5. Inter-block boundary condition between the blocks of the **DD** [DD94, Meu91]. In this artificial boundary a Dirichlet condition is imposed to the mass conservation equation (2.1) and a single iteration is performed to allow the overlapped cells to converge.

Figure 2 Inter-block boundary condition and overlapped area.

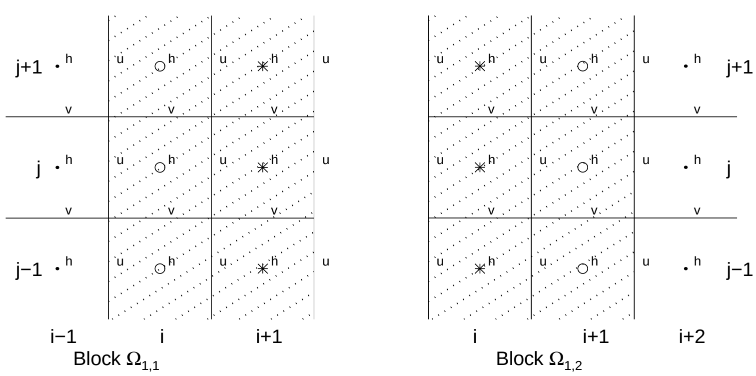

In Figure 2 the use of the overlapped region between blocks is shown. Variables marked with a $*$ are used to set boundary conditions in the the block to which they belong; variables marked with a $\circ$ are to be sent to the adjacent block for use as boundary conditions. This allows a non-blocking send between blocks, improving the performance of the model.

3 Domain Decomposition

In each block of the **DD** an **ADI** [LL75, KT92] (implicit in space, alternating directions in the horizontal and vertical successively) method is employed [LM92]. A first approximation of the data in the overlapped area between blocks, marked with a $*$ in Figure 2, is carried out using an explicit computation [CBBK94], resulting in an explicit/implicit hybrid method [DD94].

Figure 3 Example of a domain decomposition with the overlapped areas.

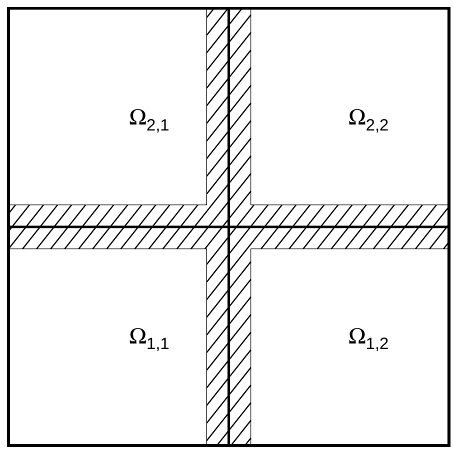

The explicit nature of the computation in the boundary between blocks puts a Courant (3.4) limitation in the time step, facing the less restrictive size of the purely implicit scheme [Roa72, Hir91, DD94]:

$$dt < \frac{dx}{\sqrt{g\overline{\overline{H}}}}, \tag{3.4}$$

where dx is the cell size, dt is the time step and $\sqrt{g\overline{\overline{H}}}$ represents an estimated tidal wave celerity in the area of the continental shelf inside the computational domain.

This scheme gives a speedup of the distributed model, due to the great magnitude of the number of cells to compute, over the serial model. The model is being tested in our virtual "parallel computer", a cluster of heterogeneous workstations, with a relatively high latency time and average bandwidth, but with an overall good cost/performance ratio. Better results could be achieved in machines with smaller latency time [LM92].

In the domain decomposition great care has been taken in the load balancing keeping in mind the number of cells in each block and the different performance of the workstations.

4 Results

For an improved calibration of the numerical model over the Río de la Plata, an area of the continental shelf must be included in the computational domain. The first test of the model is on a mesh of 400 by 400 km with 1 km grid size, giving 160,000 cells, and a 1 minute time step. A second mesh with 0.5 km resolution gives a total of 640,000 grid points, and a correspondingly reduced time step of 0.5 minutes.

In Figure 4 an application of the model to predict the speed field in low-tide condition is shown. In this figure block divisions are marked using dark lines. Figure 5 compares the surface elevation results of the model, while simulating the semi-diurnal tide component M_2[2], with the known astronomic wave component in Montevideo. The astronomic components at the coastal ports, used in the comparison and in boundary conditions, are obtained by harmonic analysis of several years surface elevation records [SOH, SHO].

Figure 4 Low-tide velocity field in the Río de la Plata.

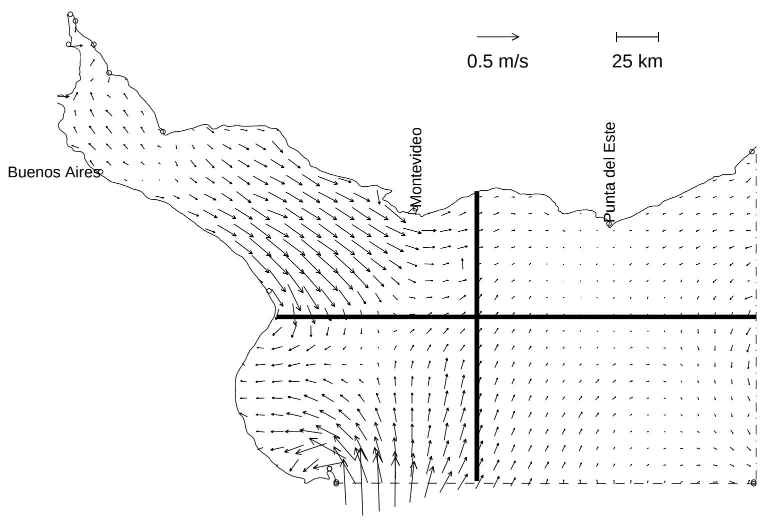

Table 1 shows the speedup of the parallelized model using 4 dedicated workstations communicating by FDDI compared to the serial model. Columns 2 and 3 pictures the Tidal Model run-time for the two meshes employed. In columns 4 and 5 of the table the run-time is measured using the Tidal Model coupled with a transport-diffusion environmental model, which overloads the workstations with a practical application, giving a better speedup in this case.

2 This is the main astronomic tide component, it has a period of 12.4206 hours and an amplitude between 0.30 and 0.10 meters in the Argentinian and Uruguayan coasts, respectively.

3 Tidal Model.

4 Tidal and Transport-Diffusion Models coupled.

Figure 5 Model results and known surface elevation for M_2 semi-diurnal tide component.

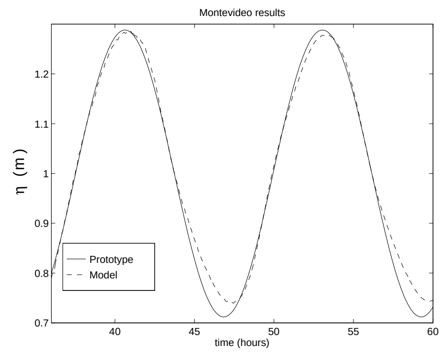

Table 1 Run time and speedup in 24 hours of simulation.

Cell size (m)	1000	500	1000	500
Number of cells	160,000	640,000	160,000	640,000
	TM[3]		TM&TD[4]	
Serial run time	57'	7h 30'	2h 00'	15h 00'
Parallel run time	22'	2h 20'	40'	4h 15'
Speedup	2.6	3.2	3.0	3.5

REFERENCES

[AL80] Arakawa A. and Lamb V. R. (1980) A potential enstrophy conserving scheme for the shallow water equations. *Monthly Weather Review* 109: 18–36.

[AQS94] Agoshkov V., Quarteroni A., and Saleri F. (1994) Recent developments in the numerical solution of shallow water equations I: boundary conditions. *Appl. Numer. Math.* 15(2): 175–200.

[Ark88] Arkawa A. (1988) *Physically-Based Modelling and Simulation of climate and climatic Change, Part-I*, chapter Finite-Difference methods in Climate Modelling, pages 79–168. Kluwer Academic Press.

[Bor85] Borche A. (1985) Modelo matemático de correntología do estuário do río Guaíba. Technical Report 12, Instituto de Pesquisas Hidráulicas da UFRGS, Porto Alegre, Brasil. In Portuguese.

[CBBK94] Cekirge H., Berlin J., Bernatz R., and Koch M. (1994) An appropiate algorithm in parallel computations for three-dimensional hydrodynamics. *Math. Comput. Modelling* 20(1): 65–84.

[DD94] Dawson C. and Dupont T. (1994) Explicit/implicit, conservative domain decomposition procedures for parabolic problems based in block centered finite differences. *SIAM J. Numer. Anal.* 31(4): 1045–1061.

[GBD+93] Geist A., Beguelin A., Dongarra J., Mancheck R., and Sunderam V. (1993) *PVM 3.0 Users's Guide and Reference Manual.* Oak Ridge National Laboratory Report.

[GK92] Gropp W. D. and Keyes D. E. (1992) Domain decomposition methods in

computational fluid dynamics. *Int. J. Numer. Meths. Fluids* 14: 147–165.
[GKV+92] Guarga R., Kaplan E., Vinzon S., Rodriguez H., and Piedracueva I. (June 1992) Aplicación de un modelo de corrientes en diferencias finitas al Río de la Plata. *Revista Latinoamericana de Hidráulica* 1(4): 93–115. In Spanish, with English abstract.
[Hir91] Hirsch C. (1991) *Numerical Computation of Internal and External Flows.* John Wiley & Sons.
[KL94] Kim C. and Lee J. (1994) A three-dimensional pc-based hydrodynamic model using an ADI scheme. *Coastal Engineering* 23: 271–287.
[KVR92] Kaplan E., Vinzon S., and Rodriguez H. (1992) Aplication of a tidal currents numerical model to the Río de la Plata. In *Hydraulic Engineering Software IV, Fluid Flow Modelling*, volume 4 of *Hydrosoft*, pages 561–573. Elsevier.
[LL75] Leendertse J. and Liu S. (1975) A three-dimensional model for estuaries and coastal seas: Vol. ii, aspects of computation. Technical report, The Rand Corp., Santa Monica, California, USA.
[LL78] Liu S. and Leendertse J. (1978) Multidimensional numerical modelling of estuaries and coastal seas. Technical report, The Rand Corp., Santa Monica, Calif.
[LM92] Leca P. and Mane L. (1992) A 3-D ADI alghoritm on distributed memory multiprocesors. In Simon H. D. (ed) *Parallel Computational Fluid Dynamics, Implementation and Results*, pages 149–165.
[Meu91] Meurant G. R. (1991) A domain decomposition method for parabolic problems. *Appl. Numer. Math.* 8: 427–441.
[Net92] Neta B. (1992) Analysis of finite elements and finite differences for shallow water equations: A review. *Mathematics and computers in simulation* 34(2): 141–161.
[Ray93] Ray R. (1993) Global ocean tide models on the eve of TOPEX/POSEIDON. *IEEE Transactions on Geos. and Rem. Sensing* 31(2): 355–364.
[RC87] Roed L. and Cooper C. (1987) A study of various open boundary conditions for wind forced barotropic numerical ocean models. In *Oceanography Series*, volume 45, pages 305–335. Elsevier.
[Roa72] Roache P. (1972) *Computational Fluid Dynamics.* Hermosa Publishers.
[Sch83] Schwiderski E. (1983) Atlas of ocean tidal charts and maps: I. the semidiurnal principal lunar tide M_2. *Marine Geodesy* 6(3-4): 219–265.
[SHO] Table des mares des grands ports du monde. Serv. Hydr. et Ocean., Paris, France. In French.
[SOH] Almanaque 1987. SOHMA., Montevideo, Uruguay. In Spanish.